Physica D 32 (1988) 423–436
North-Holland, Amsterdam

SYMMETRY-INCREASING BIFURCATION OF CHAOTIC ATTRACTORS

P. CHOSSAT[1] and M. GOLUBITSKY[2]
[1] *I.M.S.P., Université de Nice, Parc Valrose, F-06034 Nice Cedex, France*
[2] *Department of Mathematics, University of Houston, Houston, TX 77204-3476, USA*

Received 12 February 1988
Revised manuscript received 9 June 1988
Communicated by J. E. Marsden

Bifurcation in symmetric systems is typically associated with spontaneous symmetry breaking. That is, bifurcation is associated with new solutions having less symmetry.

In this paper we show that symmetry-increasing bifurcation in the discrete dynamics of symmetric mappings is possible (and is perhaps generic). The reason for these bifurcations may be understood as follows. The existence of one attractor in a system with symmetry gives rise to a family of conjugate attractors all related by symmetry. Typically, in computer experiments, what we see is a sequence of symmetry-breaking bifurcations leading to the existence of conjugate chaotic attractors. As the bifurcation parameter is varied these attractors grow in size and merge leading to a single attractor having greater symmetry.

We prove a theorem suggesting why this new attractor should have greater symmetry and present a number of striking examples of the symmetric patterns that can be formed by iterating the simplest mappings on the plane with the symmetry of the regular m-gon. In the last section we discuss period-doubling in the presence of symmetry.

0. Introduction

The coexistence of regular patterns with turbulent fluid flow seems remarkable; yet this coexistence has been observed in the Taylor–Couette system. In the experimental apparatus, fluid is contained between two concentric independently rotating, cylinders. When the outer cylinder is held fixed and the speed of rotation of the inner cylinder is increased slowly, the following sequence of states is observed: laminar Couette flow, time-independent Taylor vortices (see fig. 1(a)), time-periodic wavy vortices, two-frequency modulated wavy vortices, multi-frequency motion, broad band turbulence, and then turbulent Taylor vortices (see fig. 1(b)). See Brandstater and Swinney [1].

What is curious about this bifurcation scenario is that the changes in state, except for the last transition, all involve either a breaking of symmetry or an increase in the complexity of the dynamics. In the last transition, however, the dynamics remains complicated but the symmetries (and spatial organization) of the state increase. As pointed out to us by R. Tagg and H.L. Swinney, the symmetry in the turbulent Taylor vortex state is only on average. This symmetry, however, is clearly visible in the picture.

Admittedly, at this time, we have only a minimal understanding of this transition. Nevertheless, since it provides a motivation for the study that follows, we will attempt to describe it in more detail. In the broad band turbulent state the fluid still divides into cells but the dividing surfaces have no nontrivial symmetry. The transition to turbulent Taylor vortices involves a restoring of the planar boundary between the cells. Experimentally the turbulent Taylor vortex state might be described as adding a small 'turbulently' varying flow field to a symmetric mean field. In this sense this state has symmetry only on average.

As has been shown in several contexts in the Taylor–Couette system, however, spatial axial translation may be identified with time evolution.

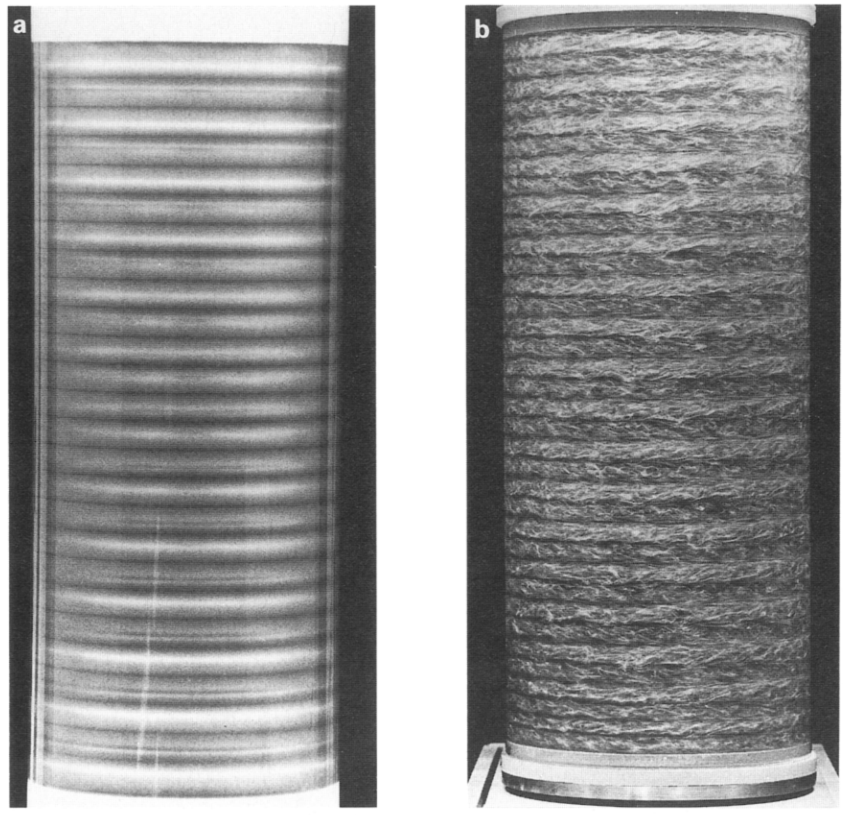

Fig. 1. Pictures from the experiments on the Taylor–Couette system (a) Taylor vortices; (b) turbulent Taylor vortices. Pictures supplied by H.L. Swinney and R. Tagg.

So that we may think of symmetry on average as being given by a time averaging process. See Case Study 6 in Golubitsky et al. [3]. We reiterate that this discussion is purely heuristic.

In this paper we discuss a rather simple method by which symmetry-increasing bifurcation can occur. Similar observations also appear in Grebogi et al. [4]. We work in the following context. Assume that the Lie group Γ acts linearly on $\mathbb{R}^n$ and that $f\colon \mathbb{R}^n \to \mathbb{R}^n$ is continuous and commutes with Γ. For an f-invariant subset A we define the symmetry of A to be the subgroup

$$\Sigma_A = \{\gamma \in \Gamma\colon \gamma A = A\}. \tag{0.1}$$

(When A consists of a single point, Σ_A is just the isotropy group of that point.)

Now assume that f depends on a parameter λ and that A_λ is an attractor for f_λ. Loosely speaking, we say that f has a *symmetry-increasing* bifurcation at $\lambda = \lambda_0$ if

(i) $\Sigma_\lambda = \Sigma_1$ for $\lambda < \lambda_0$,
(ii) $\Sigma_\lambda = \Sigma_2$ for $\lambda > \lambda_0$, and
(iii) $\Sigma_2 \supset \Sigma_1$.

Computer experiments suggest the following. Suppose for $\lambda < \lambda_0$, there is an attractor A_λ with symmetry Σ and suppose that $\rho \in \Gamma \sim \Sigma$. Then $\rho(A_\lambda)$ is also an attractor which we call a *conjugate* attractor. Suppose that as λ increases to λ_0, A_λ and $\rho(A_\lambda)$ come together and merge at λ_0. Then we find that the resulting attractor A_λ for $\lambda > \lambda_0$ has symmetries which include the group generated by Σ and ρ. In Section 1 we prove a

proposition detailing an instance where this symmetry statement can be made precise. One should note that the existence of conjugate attractors is forced by symmetry, whenever the given attractor has less than full symmetry. Therefore, the merger of attractors should occur naturally in the discrete dynamics of mapping with symmetry. Also note that the symmetry of a chaotic attractor, as we have defined it, will only be visible on average. For examples see the figures in sections 3 and 5.

The remaining sections of the paper discuss examples of merging of attractors. In section 2 we discuss the odd logistic equation (mentioned in Chossat and Golubitsky [2]). In section 3 we discuss iterates of maps with D_3 symmetry in the plane and show several different routes by which symmetry-increasing bifurcations to D_3-symmetric attractors occur. Section 5 is a show-and-tell section presenting some of the striking invariant sets that can be obtained through mergers of conjugate attractors when iterating maps of the plane with D_m symmetry for $m = 3, 5, 6, 7$ and 9. In section 4 we present a general theorem describing period doubling in the presence of symmetry and apply our results to the case of D_m symmetry. The different fixed-point and period-doubling bifurcations lead into the scenarios of symmetry-increasing bifurcations that we present in sections 3 and 5.

1. Symmetry of an attractor

Let $f: \mathbb{R}^2 \to \mathbb{R}^2$ be a mapping and let A be an invariant set under f. We feel that there are three properties of f and A that should hold if the set A is to be *observed* by computer experiment on f:

(H1) $f(A) = A$.

(H2) A has a dense orbit $T = \{z, f(z), f^2(z), \dots\}$.

(H3) A is an 'attractor', that is, there is an open neighborhood U of A such that for every $x \in U$, $\omega(x) \subset A$.

Here $\omega(x)$ denotes the ω-limit point set of x.

The computer experiment we have in mind is the following: choose an initial point x and then plot the iterates of f until the graphical image settles down. By 'settles down' we mean that the set A that appears on the screen may be reproduced by clearing the screen and continuing to plot iterates on the same orbit. We abstract this notion by (H1). In the experiment we plot the iterates of f lying on one trajectory; thus the set A that we see on the computer screen is just the 'closure' of the given trajectory. This notion is abstracted by (H2). Finally, to guard against numerical errors when determining the asymptotic shape of A, we repeat the process for different initial conditions. We abstract the idea that the set A does not depend on the initial condition x, as long as x is near enough to A, by (H3).

Proposition 1.1. Let $f: \mathbb{R}^n \to \mathbb{R}^n$ be continuous and commute with the matrix ρ. Let $A \subset \mathbb{R}^n$ be a closed subset. Assume that f and A satisfy (H1)–(H3) and

(H4) $A \cap \rho(A) \neq \varnothing$.

Then $\rho(A) = A$.

Remarks. (1) Proposition 1.1 suggests that when two conjugate attractors A and $\rho(A)$ collide, they can merge into a single attractor with symmetry containing ρ. Thus, it is *not* surprising that collisions of conjugate attractors produce attractors of greater symmetry.

(2) We note that just after the collision of attractors the dynamics consists of a point staying in one region of the new attractor for many iterates before moving on to another (conjugate) region. The issue of residence time in a region as a function of the bifurcation parameter has been discussed in Grebogi et al. [4] (in the nonsymmetric case). We do not consider this important issue here.

(3) Suppose $f: \mathbb{R}^n \to \mathbb{R}^n$ commutes with the Lie group Γ and the set A has nontrivial symmetry Σ_A. Then after the collision of conjugate attractors, we expect the symmetry of the resulting attractor to include the group generated by Σ_A and ρ. In particular, we will see examples with $\Gamma = D_m$ where both Σ_A and ρ have order 2, but

the group generated by Σ_A and ρ is all of Γ. The resulting pictures are quite striking.

(4) A simple way to see that (H4) is satisfied on a computer is to vary a parameter λ in f until $A_\lambda \cap \mathrm{Fix}(\rho) \neq \emptyset$, where

$$\mathrm{Fix}(\rho) = \{ v \in \mathbb{R}^n : \rho(v) = v \}.$$

Proof. Suppose that

$$\omega(x) = A \quad \text{for every } x \in T, \tag{1.1}$$

where T is defined in (H2). Then the validity of the proposition is seen as follows. Let U be the open neighborhood defined in (H3) and set

$$Q \equiv \rho(U) \cap U.$$

Observe that Q is open and nonempty, since $Q \supset \rho(A) \cap A \neq \emptyset$ by (H4). Since T is dense in A and $Q \cap A \neq \emptyset$, we have $Q \cap T \neq \emptyset$. Choose $x \in Q \cap T$. Since $x \in T$, (1.1) implies that $\omega(x) = A$. However, $x \in \rho(U)$ and the equivariance of f coupled with (H1) implies that $\omega(x) \subset \rho(A)$. Thus $A \subset \rho(A)$. Reversing the roles of A and $\rho(A)$ establishes that $A = \rho(A)$, as desired.

By (H3) we know that $\omega(x) \subset A$ for each $x \in T$. Thus to verify (1.1) we fix x and show that each $a \in A$ is in $\omega(x)$. If $a \in A \sim T$, then the density of T implies the existence of a sequence $f^{m_j}(x) \to a$ as $j \to \infty$. Thus $a \in \omega(x)$, as desired. When $a \in T$ however, the density of T in A does not imply the existence of a sequence of iterates of x converging to a since a is already in T.

We observe that if a is not isolated in A or if T is a periodic orbit, then such a sequence of iterates always exists. This statement is easily verified when T is periodic of period m, for $f^{mj}(x) = x$ for all j. Suppose now that a is not isolated in A, then there exists a sequence of distinct points $a_j \in A$ converging to a. Since T is dense in A we can choose iterates $f^{m_j}(x)$ such that

$$|a_j - f^{m_j}(x)| < |a_j - a|.$$

This inequality shows that $f^{m_j}(x) \neq a$ and $f^{m_j}(x) \to a$ as $j \to \infty$. Thus $a \in \omega(x)$.

Define $W = \{ a \in A : a \text{ is isolated} \}$. We claim that either

$$W = \emptyset \quad \text{or} \quad T \text{ is a periodic orbit.} \tag{1.2}$$

The discussion in the last paragraph shows that (1.2) implies (1.1). We verify (1.2) by assuming $W \neq \emptyset$ and showing that T is periodic.

Observe that $W \subset T$ since the density of T in A implies that isolated points in A must be in T. Also observe, that the continuity of f and the invariance of A under f implies that if a is not isolated in A, then $f(a)$ is not isolated in A. Recall from (H2) that T consists of iterates of the point z. The last comment shows that if z is not isolated in A, then no point in T is isolated in A. This contradicts the fact that $W \subset T$ and the assumption that $W \neq \emptyset$. Thus $z \in W$. Finally (H1) implies that there is an $a \in A$ such that $f(a) = z$. If a were not isolated in A, then z would not be in W. So a is in W and hence in T. Therefore $a = f^m(z)$ for some m. Thus $f^{m+1}(z) = z$ and T is a periodic orbit, as claimed. This verifies (1.2). ■

2. The odd-logistic equation

The only nontrivial (faithful) action of a compact group on $\mathbb{R}$ is given by $\mathbb{Z}_2 = \{1, \rho\}$ acting by $\rho x = -x$. The $\mathbb{Z}_2$-equivariant mappings are just the odd functions. Consider, as an example, the odd-logistic equation

$$f(x, \lambda) = \lambda x - x^3. \tag{2.1}$$

We discuss the asymptotic dynamics of f as λ increases. When $\lambda < 1$, the fixed point $x = 0$ is stable. At $\lambda = 1$ the fixed point loses stability and bifurcates producing two conjugate fixed points which are nonzero and stable. These fixed points then undergo periodic doubling cascades resulting in a pair of conjugate attractors A_+ and A_- each consisting of a single orbit 'filling up' parts of the real line, say $[\alpha, \beta]$ and $[-\beta, -\alpha]$. As λ is increased further β decreases and eventually be-

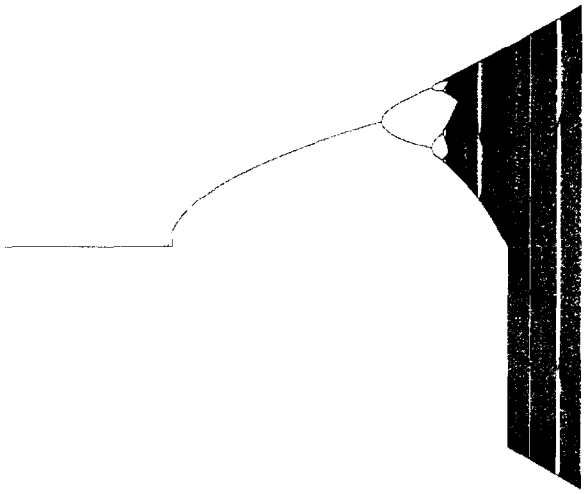

Fig. 2. Picture of iterates of the odd-logistic equation $f(x, \lambda) = \lambda x - x^3$. The picture is created by fixing λ, iterating f 100 times and then plotting the next 150 iterates of f.

comes negative. When this happens a $\mathbb{Z}_2$-symmetric attractor is produced.

The exact value of λ where this merging of attractors occurs may be calculated easily. Let x_+ be the unique positive fixed point of f and let x_c be the unique positive critical point of f. The theory of quadratic maps tells us that the positive attractor A_+ contains x_c. A necessary condition for an iterate of some point in A_+ to be negative is that $f(x_c) \geq x_+$. (To verify this remark just look at the graph of f.) The smallest value of λ where this condition can be satisfied is given by

$$f^2(x_c) = 0.$$

Since $x_c^2 = \lambda/3$, it is easy to verify that this value is

$$\lambda_c = 3\sqrt{3}/2.$$

Fig. 2 is created as follows. For a given value of λ, we iterate f for 100 points and then plot the next 150 points. We then increment λ and repeat the same process. The initial point for the incremented λ is just the terminal point of iteration by f at value λ. Note the sudden increase in symmetry of the attractor in fig. 2 at $\lambda = \lambda_c$.

3. Chaos and D_3 symmetry

The dihedral group D_m consists of all symmetries of the regular m-gon in the plane. These symmetries are generated by

$$R_m(z) = e^{2\pi i/m} z,$$
$$\kappa(z) = \bar{z}.$$

A mapping $f: V \to V$ is *equivariant* with respect to the group Γ acting on V if

$$f(\gamma v) = \gamma f(v).$$

The general D_m-equivariant mapping on $\mathbb{R}^2 \cong \mathbb{C}$ is given by

$$f(z, \lambda) = p(u, v, \lambda) z + q(u, v, \lambda) \bar{z}^{m-1}, \qquad (3.1)$$

where

$$u = z\bar{z} \quad \text{and} \quad v = (z^m + \bar{z}^m)/2. \qquad (3.2)$$

Using computer experiment, we have explored, in a haphazard way, the discrete dynamics of the following mapping:

$$f(z, \lambda) = (\alpha u + \beta v + \lambda) z + \gamma \bar{z}^{m-1}. \qquad (3.3)$$

For a complete discussion of D_m equivariants see Golubitsky et al. [2]. In this section we discuss patterns formed by symmetry-increasing bifurcations in maps with triangular symmetry, that is, in the map (3.3) when $m = 3$.

More explicitly, we choose λ to be the bifurcation parameter and we look for merging of attractors as λ is varied. We assume $\gamma \neq 0$; upon rescaling f by $af(z/a)$, we can assume $\gamma = 1$.

In our explorations we have observed many different pictures of D_3-symmetric attractors resulting from iterates of (3.3) when $m = 3$. We

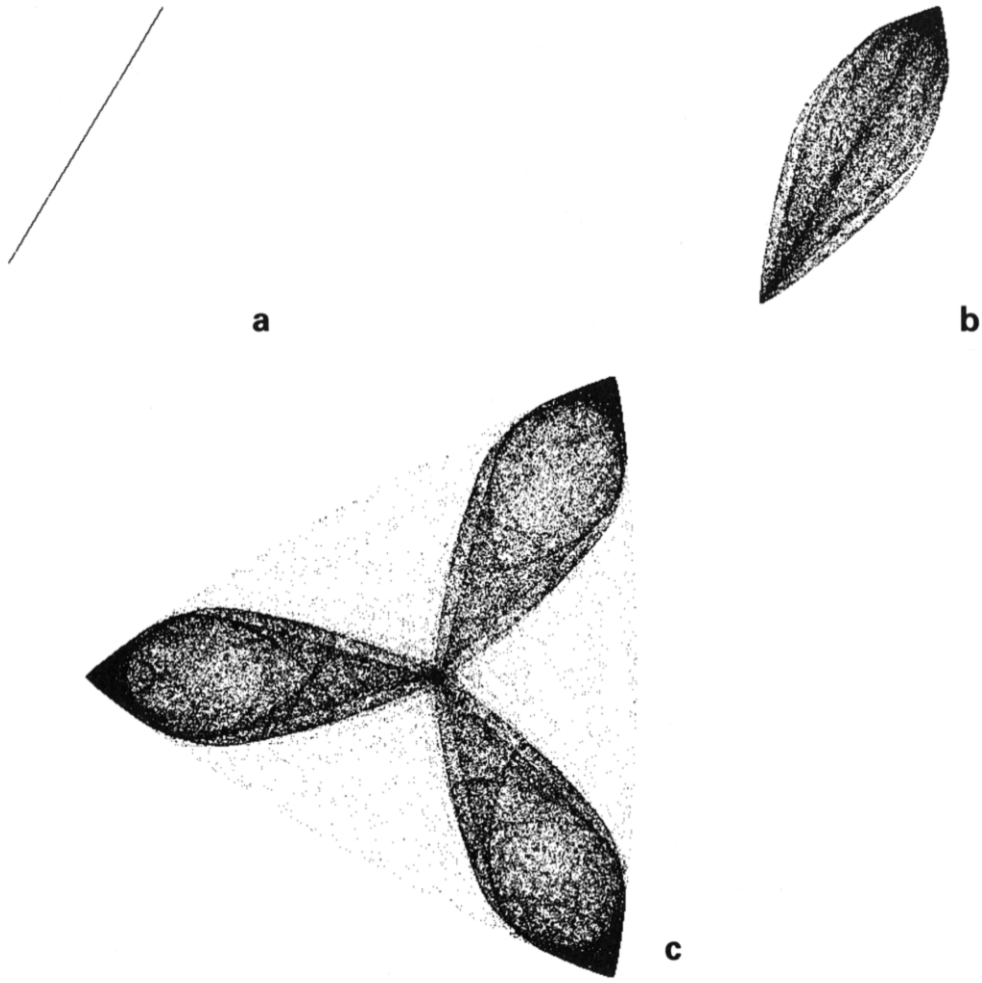

Fig. 3. Pictures of some of the transitions described in scenario 1. Numerically the transitions occur at $\lambda \approx 2.185$ and $\lambda \approx 2.27$. Here we have $\alpha = -1$, $\beta = 0$, $\gamma = -0.5$ and $m = 3$. (a) $\lambda = 2.18$, Iterates = 17889; (b) $\lambda = 2.23$, Iterates = 26559; (c) $\lambda = 2.275$, Iterates = 100706.

have, however, detected only a few types of symmetry-increasing bifurcations and these are related to the type of primary bifurcation from the D_3-invariant fixed point $z = 0$. These initial bifurcations are described in section 5. In the following scenarios, the bifurcations to and from chaotic attractors are based only on numerical evidence. Arrows indicate the typical sequence of transitions we have observed. Here $\mathbb{Z}_2(\kappa)$ denotes the two element group generated by $\kappa(z) = \bar{z}$. Recall that when Σ is a subgroup the *fixed-point subspace* is defined by

$$\mathrm{Fix}(\Sigma) = \{ z \in \mathbb{C} : \sigma z = z, \forall \sigma \in \Sigma \}.$$

Since the group acts linearly $\mathrm{Fix}(\Sigma)$ is a linear subspace. Moreover, f: $\mathrm{Fix}(\Sigma) \to \mathrm{Fix}(\Sigma)$ for any equivariant f. See Golubitsky et al. [2].

Scenario 1. (Fig. 3) $0 \to$ fixed point in $\mathrm{Fix}(\mathbb{Z}_2(\kappa))$ $\to$ chaotic 1D set in $\mathrm{Fix}(\mathbb{Z}_2(\kappa)) \to$ (eventually) chaotic $\mathbb{Z}_2(\kappa)$-symmetric set $\to D_3$-symmetric at-

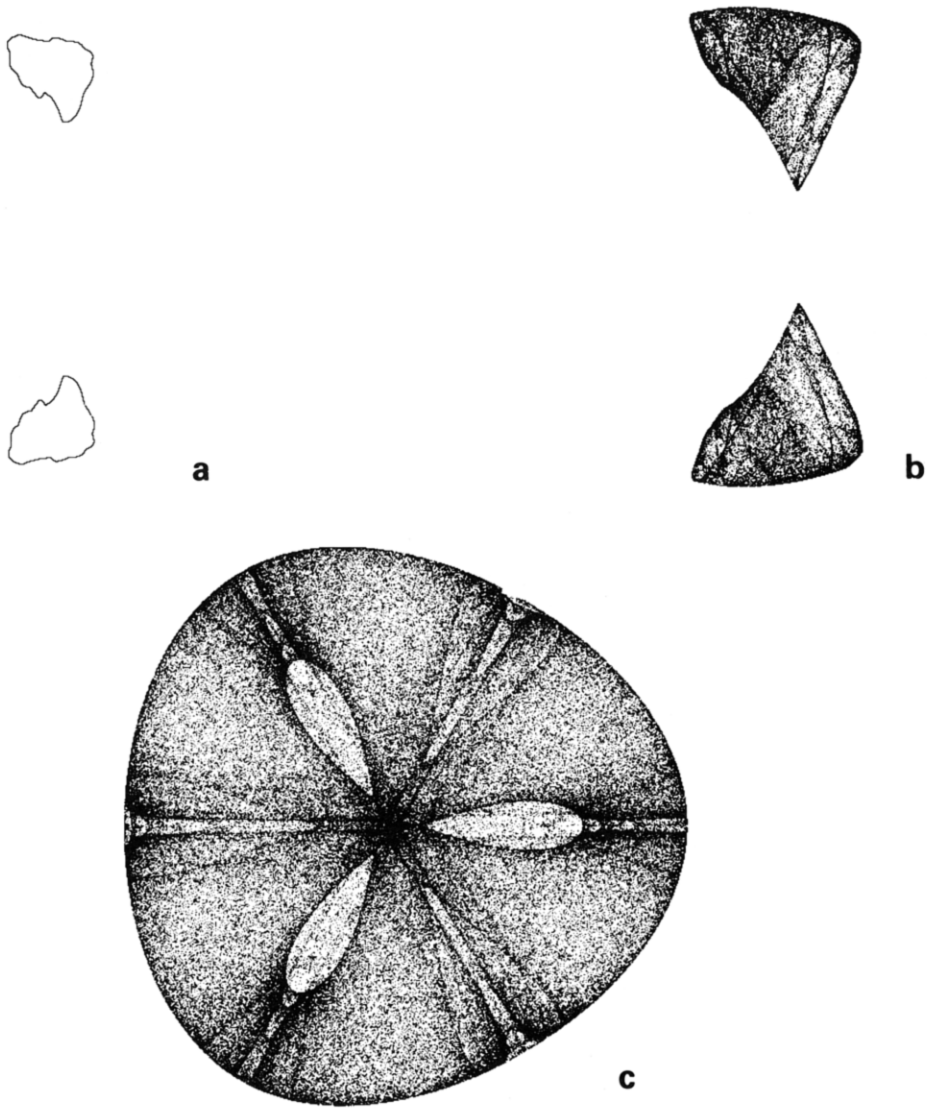

Fig. 4. Pictures of some of the transitions described in scenario 2. Numerically the transitions occur at $\lambda \approx -2.12$ and $\lambda \approx -2.375$. Here we have $\alpha = 1$, $\beta = 0$, $\gamma = 0.1$ and $m = 3$. (a) $\lambda = -2.10$, Iterates = 34113; (b) $\lambda = -2.25$, Iterates = 42714; (c) $\lambda = -2.38$, Iterates = 173182.

tractor created by a merger at 0 of conjugate $\mathbb{Z}_2(\kappa)$-symmetric attractors.

Scenario 2. (Fig. 4) 0 → fixed point in $\mathrm{Fix}(\mathbb{Z}_2(\kappa))$ → $\mathbb{Z}_2(\kappa)$-symmetric period two points → two invariant circles → $\mathbb{Z}_2(\kappa)$-symmetric chaotic attractor (obtained through merger of the invariant circles across $\mathrm{Fix}(\mathbb{Z}_2(\kappa))$) → D_3-symmetric attractor created by a merger at $\mathrm{Fix}(\Sigma)$ of conjugate $\mathbb{Z}_2(\kappa)$-symmetric attractors where Σ is a subgroup conjugate to $\mathbb{Z}_2(\kappa)$.

Remark. Since $\mathbb{Z}_2(\kappa)$ and Σ together generate D_3, we expect the resulting attractor to be D_3-symmetric.

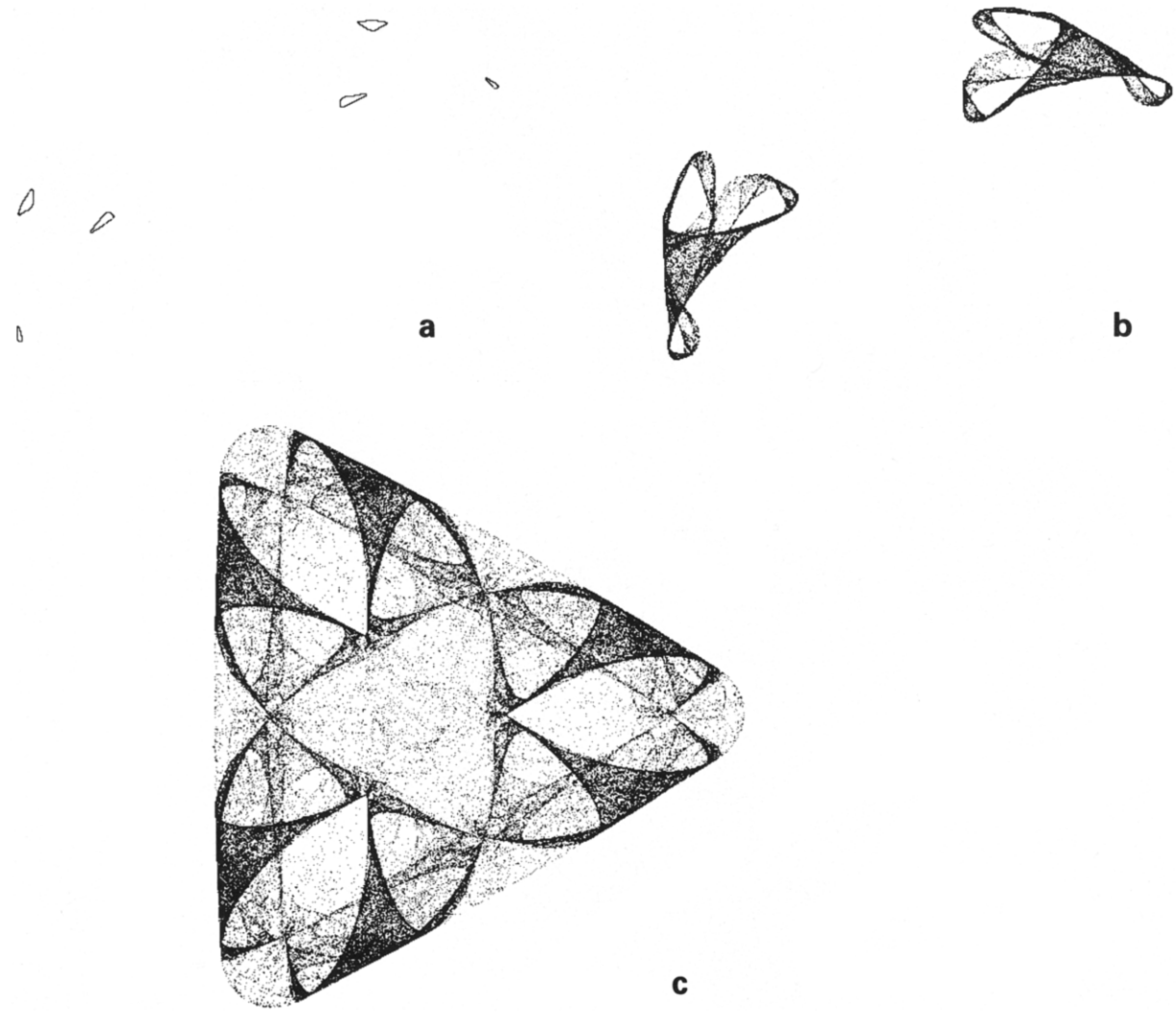

Fig. 5. Pictures of some of the transitions described in scenario 3. Numerically the transitions occur at $\lambda \approx -1.78$ and $\lambda \approx -1.80$. Here we have $\alpha = 1$, $\beta = 0$, $\gamma = 0.5$ and $m = 3$. (a) $\lambda = -1.755$, Iterates = 112617; (b) $\lambda = -1.79$, Iterates = 37327; (c) $\gamma = -1.804$, Iterates = 109949.

Scenario 3. (Fig. 5) $0 \rightarrow \mathbb{Z}_2(\kappa)$-symmetric period two points $\rightarrow$ period six points (constituting a $\mathbb{Z}_2(\kappa)$-symmetric set) $\rightarrow$ six invariant circles $\rightarrow$ $\mathbb{Z}_2(\kappa)$-symmetric chaotic attractor (obtained by merging of the invariant circles) $\rightarrow$ D_3-symmetric attractor obtained by merger of the $\mathbb{Z}_2(\kappa)$-symmetric and its conjugates at Fix(Σ), as in scenario 2.

Scenario 4. (Fig. 6) $0 \rightarrow$ period two points in Fix($\mathbb{Z}_2(\kappa)$) $\rightarrow$ period four points off of Fix($\mathbb{Z}_2(\kappa)$) $\rightarrow$ nonsymmetric chaotic attractor (a) $\rightarrow$ $\mathbb{Z}_2(\kappa)$-symmetric chaotic attractor, having a fine structure similar to the Hénon strange attractor (with a Cantor type cross section) (b) $\rightarrow$ D_3-symmetric attractor obtained by merging of the conjugate $\mathbb{Z}_2(\kappa)$-symmetric attractors at Fix(Σ), as in scenario 2 (c).

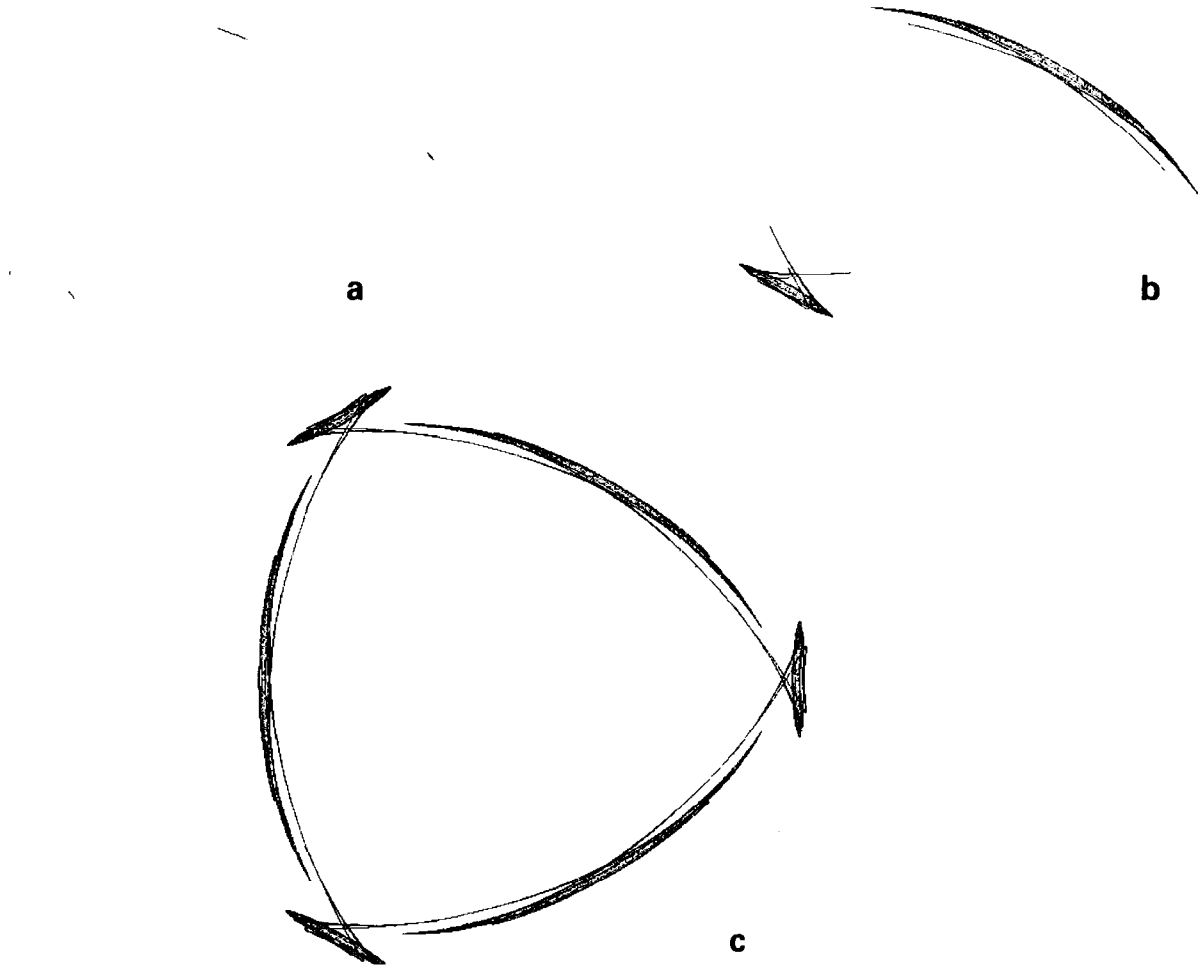

Fig. 6. Pictures of some of the transitions described in scenario 4. Numerically the transitions occur at $\lambda \approx -1.92893$ and $\lambda \approx -1.937$. Here we have $\alpha = 1$, $\beta = -0.7$, $\gamma = -0.8$ and $m = 3$. (a) $\lambda = -1.937$, Iterates = 93162; (b) $\lambda = -1.93$, Iterates = 55841; (c) $\lambda = -1.94$, Iterates = 143572.

Remark. It is remarkable that each of these scenarios leads to attractors with different forms and seemingly different structure.

Finally, we remark that the pictures here could not have been created by iterating homeomorphisms. For a homeomorphism the points x and $f(x)$ must have the same isotropy, yet in these cases the numerics show existence of points with isotropy subgroup 1 which are taken by f to a point with isotropy D_3 in the first example and to a point with isotropy $\mathbb{Z}_2(\kappa)$ in the second.

4. Period doubling and symmetry

As we mentioned in section 3 the scenarios of symmetry-increasing bifurcation we have observed on the computer all begin with symmetry-breaking bifurcation. Indeed, the broad classes we have seen begin with a stable Γ-invariant fixed point losing stability either by a symmetry-breaking bifurcation to new fixed points or a symmetry-breaking bifurcation to period two points. In this section we discuss the period two bifurcations in detail.

Let $f\colon \mathbb{R}^n \times \mathbb{R} \to \mathbb{R}^n$ be a Γ-equivariant mapping where Γ acts absolutely irreducibly on $\mathbb{R}^n$. It follows that $f(0, \lambda) = 0$ (that is, for all λ, 0 is a Γ-invariant fixed point of f) and

$$(\mathrm{d}_x f)_{0,\lambda} = \sigma(\lambda) I_n.$$

We assume that the fixed point 0 is asymptotically stable when $\lambda < 0$, that is, $|\sigma(\lambda)| < 1$, and that 0 loses stability at $\lambda = 0$. A bifurcation of fixed points occurs when $\sigma(0) = +1$ and a period-doubling bifurcation occurs when $\sigma(0) = -1$.

Bifurcation of fixed points is analogous to bifurcation of stationary points for vector fields. This issue is discussed in Chossat & Golubitsky [1988], Lemma 2.1. In particular, there is a branch of fixed points corresponding to each isotropy subgroup Σ whose fixed point space $\mathrm{Fix}(\Sigma)$ has dimension one. In the case $\Gamma = D_m$ and $n = 2$, the lattice of isotropy subgroups is:

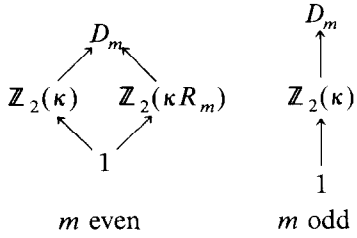

where $\mathbb{R}^2 \cong \mathbb{C}$, $\kappa(z) = \bar{z}$ and $R_m(z) = \mathrm{e}^{2\pi \mathrm{i}/m} z$. Moreover, the dimensions of $\mathrm{Fix}(\mathbb{Z}_2(\xi))$ and $\mathrm{Fix}(\mathbb{Z}_2(\kappa R_m)$ are both equal to one. Thus, there are bifurcating fixed points with a reflectional symmetry and, in fact, generically no other fixed points. (See Golubitsky et al. [2].)

For the remainder of this section we discuss the bifurcation of period two points, that is, we assume $\sigma(0) = -1$. As we remarked in Chossat and Golubitsky [4], lemma 2.2, period two points are fixed points of the second iterate $f^2 = f \circ f$. Thus there are period two points with isotropy $\mathbb{Z}_2(\kappa)$ for all m and $\mathbb{Z}_2(\kappa R_m)$ when m is even. In fact, we claim that there is also a second family of period two points when m is odd.

Using a theorem of Iooss [6], the normal form h for f commutes with the linear part of f. In this case, this means that h commutes with $-I_n$. Group theoretically, let $\mathbb{Z}_2 = \{\pm I_n\}$ and suppose $-I_n$ is not in the representation of Γ on $\mathbb{R}^n$. Then the normal form h will commute with $\Gamma \oplus \mathbb{Z}_2$. It follows from the previous discussion that the normal form will have period two points corresponding to every isotropy subgroup Σ of $\Gamma \oplus \mathbb{Z}_2$ whose fixed point subspace has dimension one. In the case of $\Gamma = D_m$ (m odd), $-I_2$ is not in D_m, and the action of $D_m \oplus \mathbb{Z}_2$ is isomorphic to the action of D_{2m}.

We address three questions:

a. Do the period two points found in the normal form h persist in the original mapping f?
b. What are the isotropy subgroups of $\Gamma \oplus \mathbb{Z}_2$ and how can we compute the dimension of the fixed point subspaces?
c. In the case of $\Gamma = D_m$, when are the bifurcating period two points asymptotically stable?

The answers to these questions are:

Theorem 4.1. Assume that Γ acts absolutely irreducibly on $\mathbb{R}^n$, that $(\mathrm{d}_x f)_{0,0} = -I_n$, and that $\dim \mathrm{Fix}(\Sigma) = 1$ for a subgroup $\Sigma \subset \Gamma \oplus \mathbb{Z}_2$. Then generically, there exists a branch of period two points for f bifurcating at the origin and tangent to $\mathrm{Fix}(\Sigma)$ at 0. If $\Sigma \subset \Gamma$, then the branch lies in $\mathrm{Fix}(\Sigma)$.

Lemma 4.2. (i) Let Σ be an isotropy subgroup of $\Gamma \oplus \mathbb{Z}_2$. Then, either $\Sigma \subset \Gamma$ or $\Sigma = \{K, I_n\} \cup \{H \sim K, -I_n\}$ where H is a subgroup of Γ, $K = \Sigma \cap \Gamma$ and the index of K in H is two.

(ii) In the latter case, $\dim \mathrm{Fix}(\Sigma) = \dim \mathrm{Fix}(K) - \dim \mathrm{Fix}(H)$.

The general mapping commuting with D_m has the form

$$f(z, \lambda) = p(u, v, \lambda) z + q(u, v, \lambda) \bar{z}^{m-1}, \qquad (4.1)$$

where $u = z\bar{z}$ and $v = z^m + \bar{z}^m$.

Proposition 4.3. There are two branches of period two points emanating from a period-doubling bifurcation with D_m symmetry, one having $\mathbb{Z}_2(\kappa)$ isotropy and the other either has $\mathbb{Z}_2(\kappa R_m)$ isotropy when m is even or is a discrete rotating wave (in the sense that $f(z) = -z$) when m is odd.

Both branches are supercritical if

$$\operatorname{sgn}(p_\lambda(0)) = -\operatorname{sgn}(p_u(0))$$

and subcritical for the opposite sign. For either branch to consist of asymptotically stable period two points it is necessary that

$$p_u(0) > 0.$$

The $\mathbb{Z}_2(\kappa)$ branch is asymptotically stable if, in addition, $\Xi > 0$ while the other branch is asymptotically stable if $\Xi < 0$, where

$$\Xi = \begin{cases} q(0) & (m \text{ even}), \\ q(0)\left[mp_u(0)q(0) + 2mp_v(0) + 2q_u(0)\right] & \\ \quad + 4q_v(0) & (m \text{ odd}). \end{cases}$$

Sketch of proof. When m is even this proposition is proved in the following manner. We write the D_m-equivariant mapping $g = f \circ f - \mathrm{id}$ in the form (4.1), namely,

$$g(z, \lambda) = P(u, v, \lambda)z + Q(u, v, \lambda)\bar{z}^{m-1}.$$

Note that period two points for f correspond to zeroes of g. So we can use standard steady state bifurcation techniques, such as in Golubitsky et al. [2], to obtain the direction of branching and stability of solutions in terms of the Taylor expansion of P and Q. The final step is to determine these Taylor coefficients in terms of p and q. The results are recorded in proposition 4.3.

When m is odd, the normal form of D_m-equivariant mappings at a period-doubling bifurcation is D_{2m}-equivariant and the even m part of proposition 4.3 applies to the normal form mapping. In addition to those computations needed for the proof of Proposition 4.3, the only computations that are necessary when m is odd consist of calculations interpreting the coefficients of P and Q in terms of the Taylor expansion of (4.1). This type of calculation is typical of normal form calculations (and no less painful) and is, in this sense, straightforward. ■

Sketch of proof of theorem 4.1. Let f_N be the normal form of f up to order N. Thus, $f_N(-x, \lambda) = -f_N(x, \lambda)$. Write $g = f \circ f - \mathrm{id}$ and recall that zeroes of g are period two points for f. We now discuss the zeroes of g.

The absolute irreducibility of Γ acting on $\mathbb{R}^n$ implies that

$$(\mathrm{d}_x f)_{(0,\lambda)} = \sigma(\lambda) I_n,$$

where $\sigma(0) = -1$. Now use Taylor's theorem to decompose g into

$$g(x, \lambda) = g_N(x, \lambda) + R_N(x, \lambda),$$

where $g_N(\cdot, \lambda)$ is a polynomial of degree N commuting with $\Gamma \oplus \mathbb{Z}_2$ and R_N is the remainder. Observe that $-\mathrm{id} \notin \Sigma$ and therefore $g_N|\mathrm{Fix}(\Sigma)$ is odd in x. In particular,

$$g_3(tv, \lambda)|\mathrm{Fix}(\Sigma) = \left(\sigma^2(\lambda) - 1 + bt^2\right)tv,$$

where v is a nonzero vector in $\mathrm{Fix}(\Sigma)$. Under the generic nondegeneracy conditions $\sigma'(0) \neq 0$ and $b \neq 0$, there is then a unique branch of nontrivial zeroes of g_N bifurcating from the origin.

At this point we would like to apply the implicit function theorem to conclude that there is a unique branch of zeroes of g tangent to $\mathrm{Fix}(\Sigma)$ at the origin. There is a difficulty. To apply the implicit function theorem we need to know that $(\mathrm{d}_x h)_{(0,0)}$ is nonsingular, where h is $g|\mathrm{Fix}(\Sigma) \times \mathbb{R}$. This matrix, however, may be forced by symmetry to be singular. To avoid this difficulty, we instead choose N large enough so that

$$\det(\mathrm{d}_x g_N)_{(x(\lambda),\lambda)} \neq 0,$$

where $x(\lambda)$ parametrizes the unique branch of nontrivial zeroes of $g_N|\mathrm{Fix}(\Sigma)\times\mathbb{R}$. (This difficulty occurs, for example, in the case of D_m when m is odd.)

Now we can use the implicit function theorem by writing $x = x(\lambda) + Y$ and rescaling each coordinate in a basis formed by the eigenvectors (or generalized eigenvectors) of $(\mathrm{d}_x g_N)_{(x(\lambda),\lambda)}$. The resulting system of equations will have nonsingular Jacobian at $(Y,\lambda) = (0,0)$. An alternate method would be to apply the theory of normally hyperbolic sets in Hirsch et al. [5]. (For a fixed point, normal hyperbolicity is just the assumption of a nonsingular derivative for the 'unperturbed' map g_N along the branch. Then R_N can be viewed as a smooth 'perturbation' of g_N and the main theorem of Hirsch et al. gives the existence of a zero of g near $x(\lambda)$. ■

Proof of lemma 4.2. (i) Assume that $\Sigma \not\subset \Gamma$. Let π: $\Gamma \oplus \mathbb{Z}_2 \to \Gamma$ be projection; note that $\ker \pi = \mathbb{Z}_2$. As observed above an isotropy subgroup cannot contain $-\mathrm{id}$. Therefore, $H = \pi(\Sigma)$ is isomorphic to Σ. Let $K = \Sigma \cap \Gamma$. Then the index of K in H is two since the index of K in Σ is two. In particular, $\Sigma = \{K, \mathrm{id}\} \cup \{H \sim K, -\mathrm{id}\}$.

(ii) The following trace formula holds for any isotropy subgroup Σ:

$$\dim \mathrm{Fix}(\Sigma) = \frac{1}{|\Sigma|}\sum_{\sigma\in\Sigma}\mathrm{tr}(\sigma),$$

where $|\Sigma|$ is the number of elements in Σ. Cf. Golubitsky et al. [2], theorem XIII, 3.2. A similar formula holds for continuous Lie groups. Using (i) we can write

$$\dim \mathrm{Fix}(\Sigma) = \frac{1}{|\Sigma|}\left[\sum_{\sigma\in K}\mathrm{tr}(\sigma) + \sum_{\sigma\in\{H\sim K,\,-\mathrm{id}\}}\mathrm{tr}(\sigma)\right].$$

But the second summand equals

$$-\sum_{\sigma\in H\sim K}\mathrm{tr}(\sigma) = -\sum_{\sigma\in H}\mathrm{tr}(\sigma) + \sum_{\sigma\in K}\mathrm{tr}(\sigma).$$

Therefore, using $|H| = |\Sigma|$ and $|K| = |\Sigma|/2$, we derive the desired formula. ■

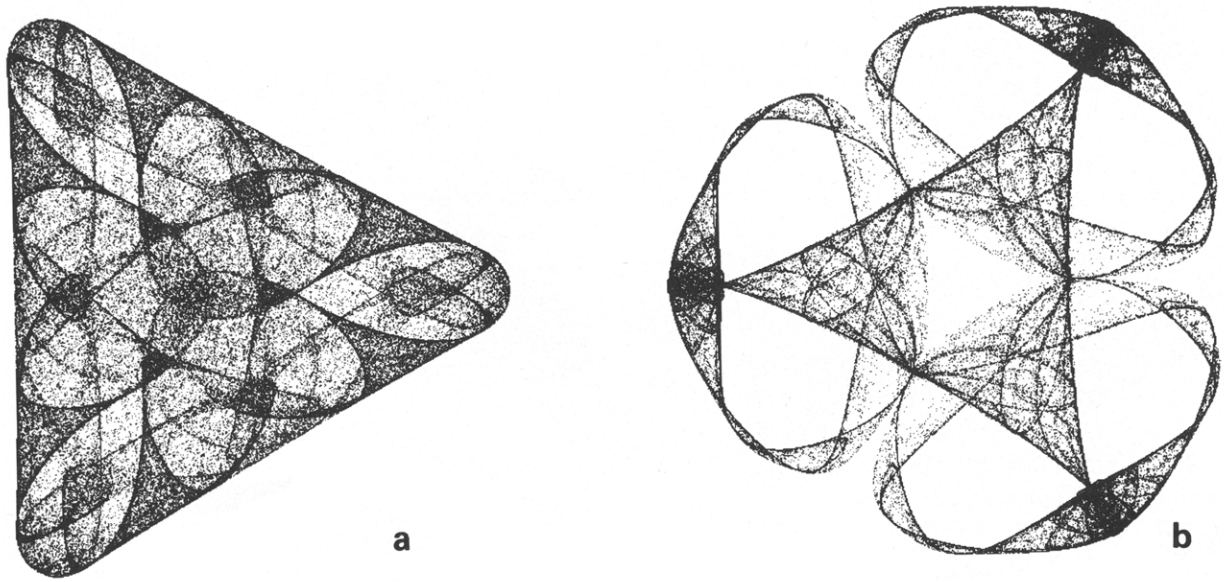

Fig. 7. Pictures of symmetric attractors with triangular symmetry. (a) $\lambda = -1.75$, $\alpha = 2.00$, $\beta = -0.20$, $\gamma = 1.00$, $m = 3$, Iterates = 137435; (b) $\lambda = 1.52$, $\alpha = -1.00$, $\beta = 0.10$, $\gamma = -0.80$, $m = 3$, Iterates = 156879.

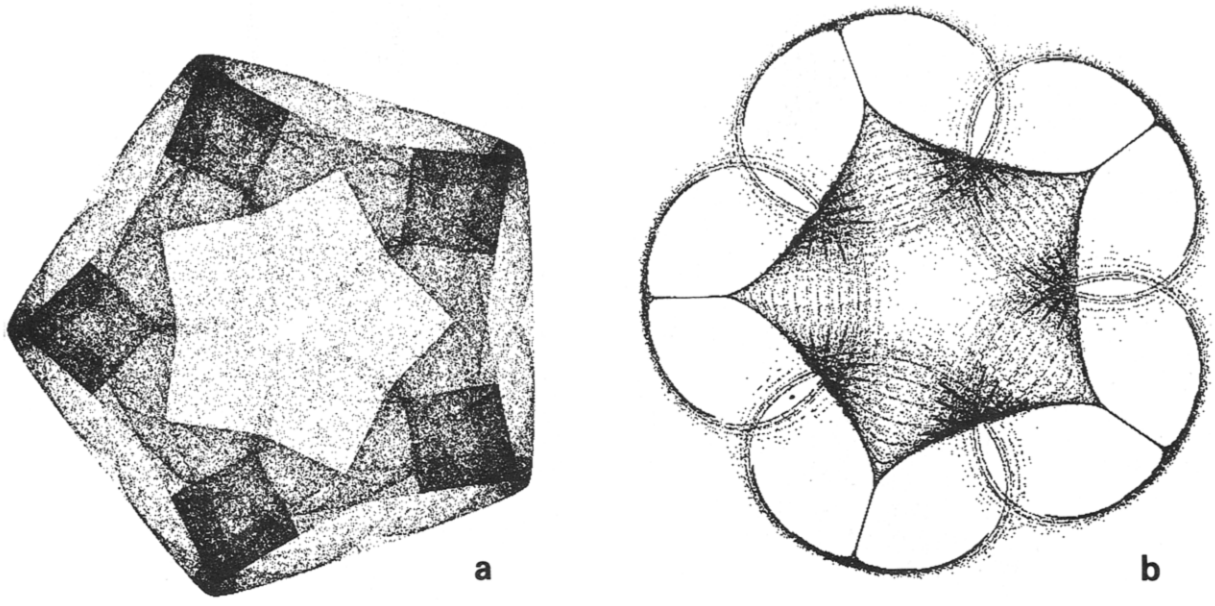

Fig. 8. Pictures of symmetric attractors with pentagonal symmetry. (a) $\lambda = 2.60$, $\alpha = -2.00$, $\beta = 0.00$, $\gamma = -0.50$, $m = 5$, Iterates = 116241; (b) $\lambda = -1.30$, $\alpha = -1.00$, $\beta = 0.10$, $\gamma = -0.80$, $m = 5$, Iterates = 262114.

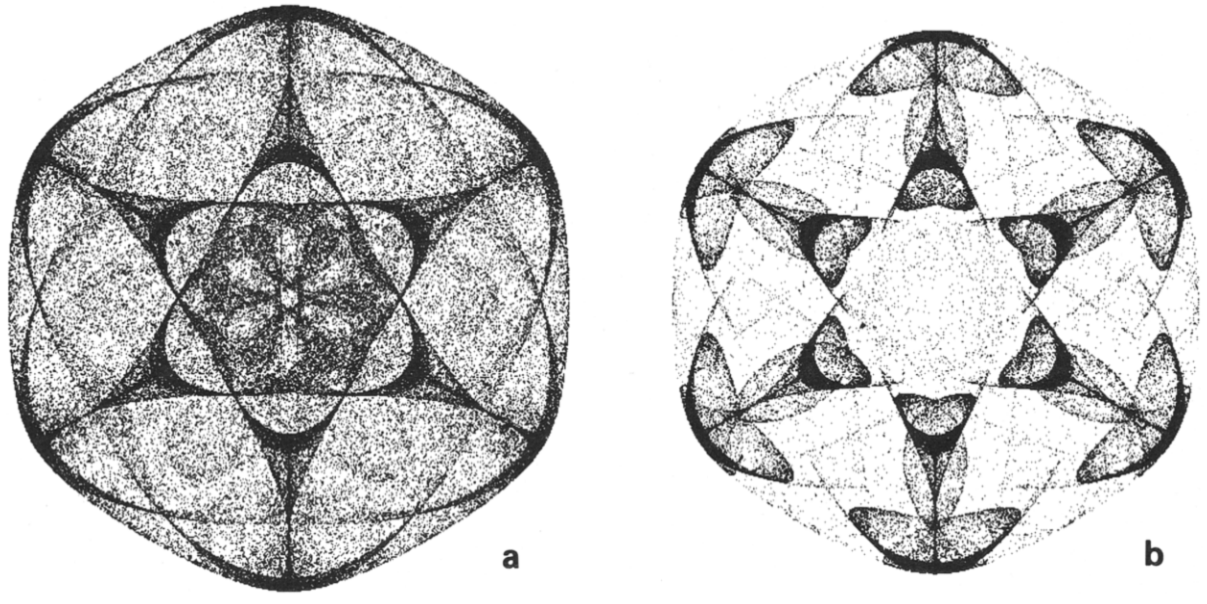

Fig. 9. Pictures of symmetric attractors with hexagonal symmetry. (a) $\lambda = -2.70$, $\alpha = 5.00$, $\beta = 2.00$, $\gamma = 1.00$, $m = 6$, Iterates = 143943; (b) $\lambda = -2.585$, $\alpha = 5.00$, $\beta = 2.00$, $\gamma = 1.00$, $m = 6$, Iterates = 150368.

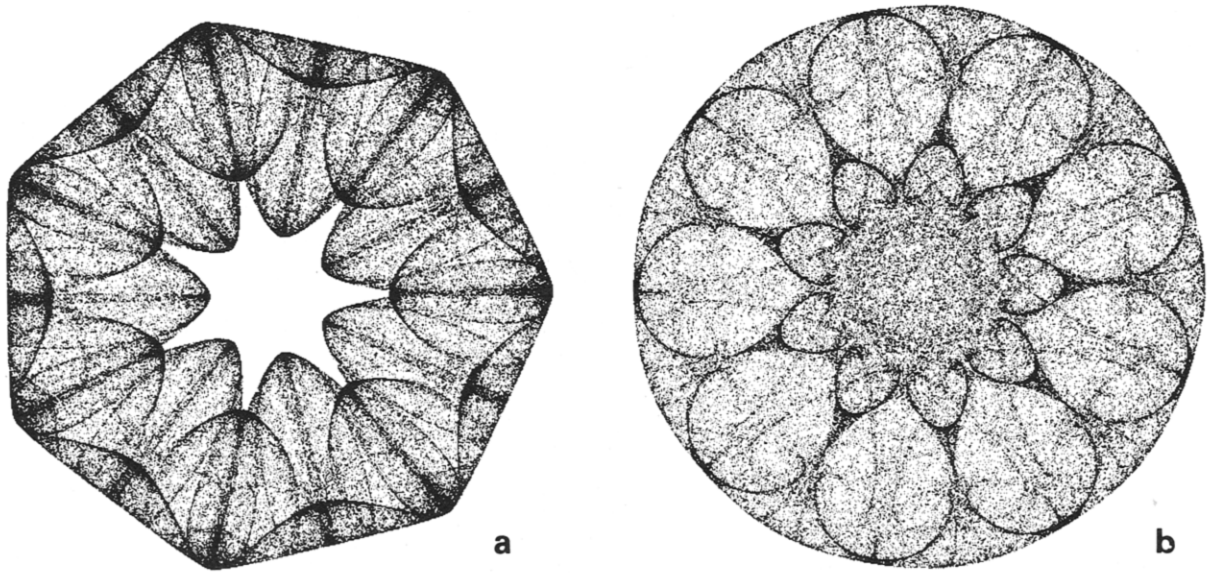

Fig. 10. Pictures of symmetric attractors with higher symmetry. (a) $\lambda = -2.065$, $\alpha = 1.00$, $\beta = 0.04$, $\gamma = 0.10$, $m = 7$, Iterates = 175119; (b) $\lambda = -2.60$, $\alpha = 4.00$, $\beta = 2.00$, $\gamma = 1.00$, $m = 9$, Iterates = 116495.

5. Selected pictures with D_m symmetric attractors

We have collected here some of the attractors that we have seen in the dynamics of mappings with D_m symmetry, when $m = 3, 5, 6, 7, 9$. These pictures are given in figs. 7–10, respectively. All attractors are shown only after symmetry-increasing bifurcations have occurred. All are obtained by iterating equation (3.3).

Acknowledgements

This research was supported in part by the ACMP program of DARPA, by NASA-Ames Grant NAG 2-432 and by NSF Grant DMS-8402604. P.C. would like to thank the Department of Mathematics of the University of Houston for a visiting position during which time this research was completed. We are grateful to John David Crawford for a number of helpful remarks.

References

[1] A. Brandstater and H.L. Swinney, Strange attractors in weakly turbulent Couette–Taylor flow, Phys. Rev. A 35 (1987) 2207–2220.
[2] P. Chossat and M. Golubitsky, Iterates of maps with symmetry, SIAM J. Math. Anal. 19, No. 6, (1988), to appear.
[3] M. Golubitsky, I.N. Stewart and D. G. Schaeffer, Singularities and Groups in Bifurcation Theory, vol. II, Appl. Math. Sci. Ser. 69 (Springer, New York, 1988).
[4] C. Grebogi, E. Ott, F. Romeiras and J.A. Yorke, Critical exponents for crisis induced intermittency, Phys. Rev. A 36 (1987), 5365–5380.
[5] M.W. Hirsch, C.C. Pugh and M. Shub, Invariant Manifolds, Lect. Notes in Math. 583 (Springer, New York, 1977).
[6] G. Iooss, Formes normales d'application – characterisation globale et methode de calcul, Université de Nice, preprint (1987).